analytical chemistry

Article

pubs.acs.org/ac

Evaluating Droplet Digital Polymerase Chain Reaction for the Quantification of Human Genomic DNA: Lifting the Traceability Fog

Margaret C. Kline and David L. Duewer*

Materials Measurement Laboratory, National Institute of Standards and Technology, Gaithersburg, Maryland 20899, United States

Supporting Information

ABSTRACT: Digital polymerase chain reaction (dPCR) end point platforms directly estimate the number of DNA target copies per reaction partition, λ, where the partitions are fixed-location chambers (cdPCR) or aqueous droplets floating in oil (ddPCR). For use in the certification of target concentration in primary calibrant certified reference materials (CRMs), both λ and the partition volume, V, must be metrologically traceable to some accessible reference system, ideally, the International System of Units (SI). The fixed spatial distribution of cdPCR chambers enables real-time monitoring of PCR amplification. Analysis of the resulting reaction curves enables validation of the critical dPCR assumptions that are essential for establishing the SI traceability of λ. We know of no direct method for validating these assumptions for ddPCR platforms. The manufacturers of the cdPCR and ddPCR systems available to us do not provide traceable partition volume specifications. Our colleagues at the National Institute of Standards and Technology (NIST) have developed a reliable method for determining ddPCR droplet volume and have demonstrated that different ddPCR reagents yield droplets of somewhat different size. Thus, neither dPCR platform by itself provides metrologically traceable estimates of target concentration. We show here that evaluating split samples with both cdPCR and ddPCR platforms can transfer the λ traceability characteristics of a cdPCR assay to its ddPCR analogue, establishing fully traceable ddPCR estimates of CRM target concentration.

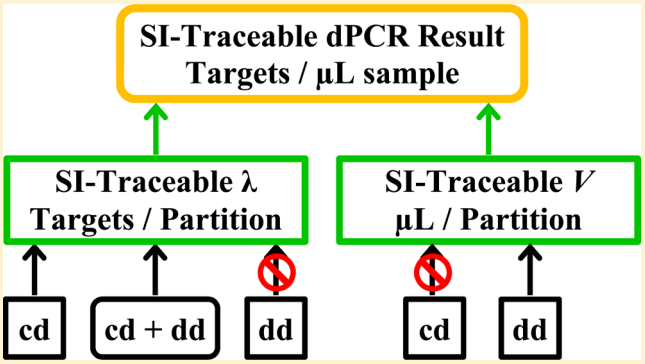

Over the past decade, digital polymerase chain reaction (dPCR) end point systems have become widely used tools for providing "absolute DNA quantification" without the need for a DNA calibrant. The several dPCR platforms that are now commercially available can be classified as chamber dPCR (cdPCR), where the polymerase chain reaction (PCR) takes place in a panel of nominally same-volume chambers, or droplet dPCR (ddPCR), where the PCR reaction takes place in nominally same-volume droplets immersed in an oil matrix.

In addition to the usual PCR need for specificity and efficiency, the crucial assumptions for successful dPCR assays are that (1) the number of DNA targets in a sample is such that, when dispersed into the dPCR reaction partitions (chamber or droplet), some partitions contain no target (negative partitions) and some partitions contain at least one target (positive partitions), (2) the targets are randomly dispersed into the partitions, (3) any partition that contains at least one target will be detected, and (4) targets migrate independently of one another.[1]

For estimating the target concentration in a sample (C), the essential dPCR quantities are the number of negative partitions (N_{neg}), the total number of partitions (N_{tot}), the mean partition volume (V), and the overall dilution factor (F, the volume fraction of sample in the reaction mixture). The mean number of targets per partition is estimated as the Poisson-transformed fraction of negative droplets, $\lambda = -\ln(N_{neg}/N_{tot})$. The concentration of targets in the sample is then $C = \lambda/(FV)$.

To help ensure that measurement results can be validly compared over time and place, results need to be metrologically traceable[2] to an accessible, internationally recognized reference system such as the International System of Units (SI).[3] Traceability is a fundamental requirement for all certified values delivered by a certified reference material (CRM). Given estimates of the values and uncertainties in each of the critical quantities, if an assay satisfies the critical dPCR assumptions then dPCR estimates of target concentration can be metrologically traceable to the SI through the natural unit count-one[4] and the derived SI unit microliter (μL).

Assays developed for quantitative real-time PCR are not necessarily suited for use with dPCR platforms, particularly those that intentionally or otherwise amplify targets at more than one locus. However, assays can be successfully designed and optimized for both cdPCR and ddPCR,[5,6] although the optimal amplification conditions for one platform may not be optimal for another.[7]

Received: January 19, 2017
Accepted: March 27, 2017
Published: March 28, 2017

ACS Publications

This article not subject to U.S. Copyright. Published 2017 by the American Chemical Society

DOI: 10.1021/acs.analchem.7b00240
Anal. Chem. 2017, 89, 4648−4654

End point assays are expected to be most precise when the number of targets per partition, λ, is about 1.6.[1,8] However, precision is not a sharp function of λ and the greater the number of partitions used per sample, the greater the range of target concentrations that can be precisely evaluated. While establishing an appropriate dilution factor, F, requires having approximate knowledge of the expected concentration of targets in a sample and the partition volume, V, appropriate dilution protocols for both cdPCR and ddPCR platforms can be established with a few trial-and-error measurements.

Because cdPCR platforms have fixed geometries the pattern of light/dark chambers within a panel at the end point cycle (see Supporting Information Figure S2) enables evaluating whether the targets were randomly distributed.[9] Real-time cdPCR (rt-cdPCR) systems visualize a signal proportional to the quantity of the PCR reaction product (amplicon) in each chamber at the completion of each PCR cycle (see Figure 1 and Supporting Information Figure S3.) The shape of these reaction curves reveals if all positive chambers efficiently amplify with the same kinetics. The distribution of crossing thresholds (Cts), the interpolated amplification cycle at which a reaction curve exceeds a user-defined intensity threshold, enables determining if all targets are likely to have been detected. The cumulative Ct distribution (ogive) embeds information about early events in the PCR process,[7] ideally including whether the targets migrated independently. Ogives for assays that very efficiently amplify the target sequence in the original DNA, the first-generation long amplicons, and the second-generation short amplicons can be used to verify that the targets are Poisson-distributed (see Supporting Information Figure S4.) At least one such assay must be available to evaluate this independence assumption.

While rt-cdPCR assays can thus be appropriately validated, for the cdPCR system that we currently use neither the manufacturer nor other authoritative party certifies the chamber volume. Given the complex geometry of the microfluidic chambers and the elasticity of the matrix that contains them, our colleagues at the National Institute of Standards and Technology (NIST) who specialize in microscale measurements[10] believe that accurate measurements of the reaction-accessible working volume in chamber systems would be, at best, difficult and expensive. Without authoritative values of chamber volume, V, cdPCR systems cannot provide metrologically traceable estimates of target concentration.

The reverse situation holds for ddPCR systems. Our colleagues recently developed a robust and relatively inexpensive method for certifying the mean volume of the nominally 100 μm diameter droplets of concern to us.[10] Using this method they have provided certified values of droplet volume and demonstrated that two of the available proprietary reagents yield droplets that differ in volume by more than 4%.[10] However, ddPCR systems do not follow the amplification course of individual droplets but classify droplets on the basis of signal intensity after the last amplification cycle. Therefore, evaluation of the PCR reaction curves for validation of the critical dPCR assumptions used with rt-cdPCR is not available for ddPCR. Further, while the negative and positive droplet intensities are ideally unambiguously different, in practice there are often ddPCR droplets of intermediate intensity that complicate classification (see Figure 2).

It is common practice to display ddPCR droplet signal intensity as a function of "event number" (within each sample, the droplet counting order), with negative droplets visualized as a band of low fluorescence intensity dots and positives as a band of considerably greater intensity. In these displays, intermediate-intensity droplets appear to be "raining down" from a cloud of positives and hence are often referred to as "rain". However, since the fluorescence intensity of a positive partition rises as amplification proceeds and more amplicon is produced, we believe that a more informative metaphor for these intermediate-intensity droplets is "fog".

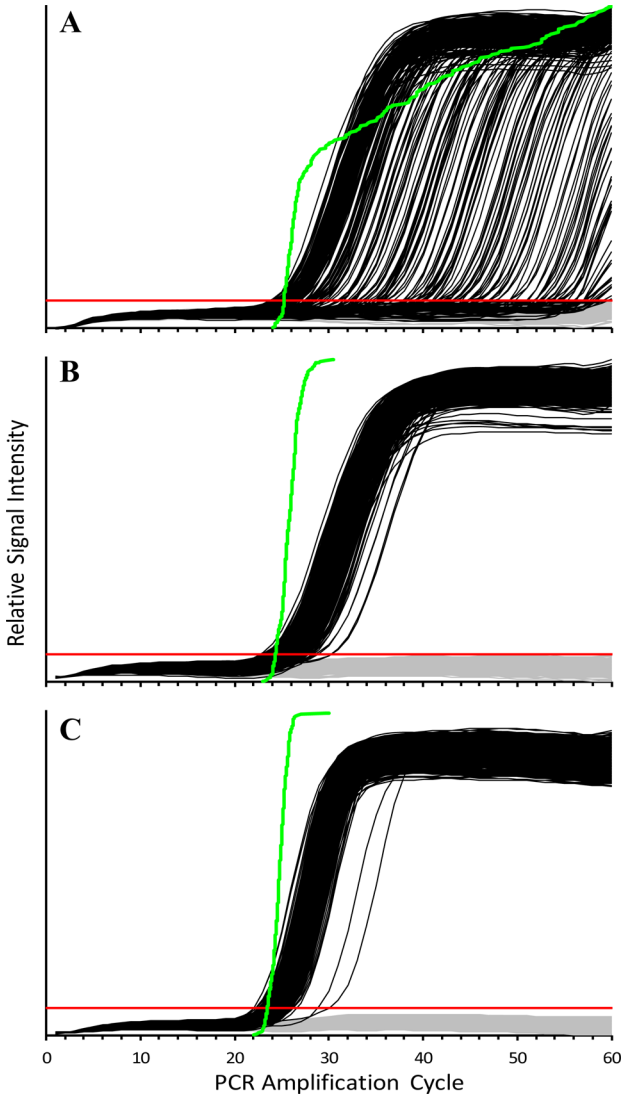

Figure 1. rt-cdPCR reaction curves for pBR322 plasmid with the 1332 assay, displaying the relative fluorescence intensity of chambers in representative 48.770 cdPCR panels as functions of PCR amplification cycle: (A) supercoiled plasmids using the GE master mix, (B) linearized plasmids using the GE master mix, and (C) supercoiled plasmids using the MZ master mix. The thin black sigmoidal curves display reaction curves for positive chambers; gray curves display signals for negative chambers. The red horizontal line denotes the empirical intensity threshold used to discriminate positive from negative chambers. The thick green sigmoidal curve is the cumulative distribution of the cycle at which the reaction curves cross the threshold. There were at most two positive chambers for nontemplate control (NTC) samples with either master mix.

While the validation approaches of the critical dPCR assumptions used with rt-cdPCR assays are not directly available for ddPCR, it is possible to demonstrate that cdPCR and ddPCR estimates of λ are concordant when the

DOI: 10.1021/acs.analchem.7b00240
Anal. Chem. 2017, 89, 4648−4654

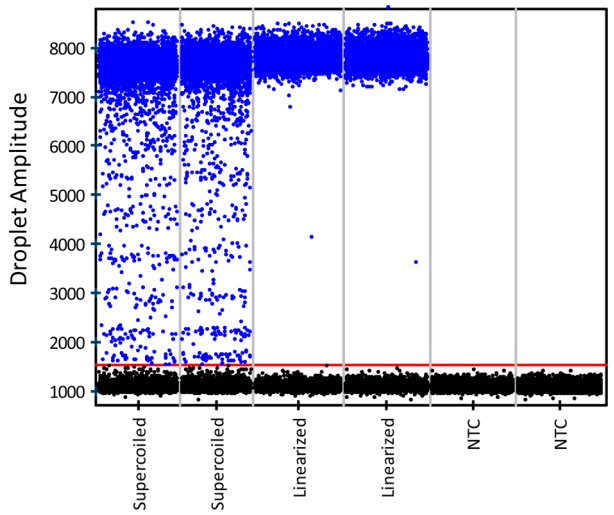

Figure 2. ddPCR droplet fluorescence intensity for the pBR322 plasmid with the 1332 assay, displaying ddPCR droplet fluorescence intensities for two representative wells each of supercoiled plasmid, linearized plasmid, and nontarget control (NTC) samples after 60 amplification cycles. Black specks denote droplets classified as negative. Blue specks denote droplets classified as positive or fog. The red horizontal line represents the intensity threshold used to classify negative droplets. The gray vertical lines mark the well boundaries.

fog droplets are properly accounted for. Using split samples over a wide range of concentrations, we argue here that the validity of the critical dPCR assumptions for a given ddPCR assay can be established through comparison of results with those from its rt-cdPCR analogue. When so validated and used with traceable estimates of V and F, concentration estimates from ddPCR assays can be confidently asserted as metrologically traceable and fit for use in CRM certification. This traceability can then be extended to results of more routine quantitative PCR assays though appropriate calibration.

MATERIALS AND METHODS

Sample Materials and PCR Assays. *Plasmid DNA.* To evaluate the sources of fog with a well-characterized small DNA genome,[11] we used pBR322 plasmid from *Escherichia coli* RRI (Sigma-Aldrich Corporation, product no. D4904.) This circular double-stranded DNA has 4363 base pairs (bp) for a molecular mass of 2.9×10^6 g/mol. The plasmid was supplied at a stated concentration of 0.5 μg plasmid DNA/μL in a 10 mmol/L tris(hydroxymethyl)aminomethane HCl (Tris), 1 mmol/L ethylenediaminetetraacetic acid (EDTA), pH 8.0 storage buffer. Four sequential volumetric dilutions into 10 mmol/L Tris, 0.1 mmol/L EDTA, pH 8.0 (TE^{-4}) buffer were used to achieve a suitably dilute master solution: 400 fg of plasmid DNA/μL nominally providing about 90 000 targets/μL. Two sets of pBR322 samples were prepared, one of the native supercoiled plasmid and a second of plasmid linearized using the EcoR I restriction enzyme (New England Biolabs, Ipswich, MA). See the Supporting Information for procedural details.

All plasmid dPCR results reported here were obtained using the NIST-developed 1332 assay. This assay produces a second-generation amplicon of 69 bp; the assay is fully described in the Supporting Information.

Human Genomic DNA. To evaluate fog sources with large DNA targets, we used the previously described multisource female NIST2 double-stranded genomic DNA in TE^{-4} buffer.[12] The NIST2 master stock solution was prepared in 2006; as of 2015 gel electrophoresis indicated that the average fragment length in this solution was greater than 48 502 bp. The human haploid genome consists of approximately 3.2×10^9 bp spread across 23 chromosomes for a total molecular mass of 2.0×10^{12} g/mol. The sample solution we used was prepared to have 13.5 ng human genomic DNA/μL providing about 4000 targets/μL.

All measurements reported here were obtained with four previously described NIST-developed assays,[12] each targeting unique sites on different chromosomes: 22C3 (chr 22), ND6 (chr 6), NEIF (chr 2), and NR4Q (chr 4). The second-generation amplicons for these assays are 78, 82, 83, and 67 bp, respectively.

dPCR Systems and PCR Master Mixes. *Chamber Digital PCR (cdPCR).* We use a Fluidigm BioMark (South San Francisco, CA) rt-cdPCR assay system with BioMark 48.770 digital arrays. Each analysis uses a disposable microfluidic device ("chip") containing 48 panels each with 770 reaction chambers. The manufacturer originally stated every chamber had a nominal volume of 0.85 nL but has recently revised this to 0.75 nL. The BioMark system monitors fluorescence intensity in all reaction chambers at the completion of each amplification cycle, enabling determination of λ at any intermediate end point as well as at the final amplification cycle. Any PCR master mix that contains the passive reference dye ROX can be used with this system.

The premixed amplification TaqMan Gene Expression master mix (GE, Applied Biosystems, catalog no. 4369016) was used for both the plasmid and human genomic samples. In addition to GE, the plasmid samples were evaluated with Molzym Mastermix 16S Basic, DNA-free (MZ, CaerusBio, Downingtown, PA, part no. S 40 0100). This MZ master mix does not contain the ROX reference dye but is compatible with ROX added to the total reaction mixture: see Supporting Information Table S2 for reaction mixture preparation. MZ contains a proprietary PCR enhancer for high G + C content targets and has been shown to efficiently amplify supercoiled pBR322 DNA.[13]

Droplet Digital PCR (ddPCR). We use a QX200 ddPCR system (Bio-Rad, Hercules, CA) where aqueous droplets are generated in an oil matrix within disposable microfluidic cartridges. After generation, the droplets from each sample are transferred into a separate well of a 96-well plate. Once all samples are transferred, the plate is thermocycler-amplified. After the final amplification cycle, the 96-well plate is manually transferred to a reader which sequentially aspirates most of the droplets in each well and determines their individual intensities. The manufacturer has used nominal droplet volumes of 0.85 and 0.91 nL in different versions of their software. Droplets having a diameter outside manufacturer-set limits are rejected and not counted. Typically, 10 000−20 000 droplets are counted per well. Only Bio-Rad proprietary master mixes can be used with this system.

The Supermix for Probes (no dUTP) (Bio-Rad, Hercules, CA, P/N 1863024) was used for both the plasmid and human genomic assays. None of the Bio-Rad master mixes commercially available at the time of this study contained a PCR enhancer equivalent to that in the MZ master mix.

Computation. rt-cdPCR reaction curves were exported from the Fluidigm Digital PCR analysis tool provided by the manufacturer into a spreadsheet-based analysis system for further manipulation. ddPCR droplet intensities were exported

DOI: 10.1021/acs.analchem.7b00240
Anal. Chem. 2017, 89, 4648−4654

from the QuantaSoft software provided by the manufacturer into a spreadsheet-based analysis system for further manipulation.

RESULTS AND DISCUSSION

Fog and Target Accessibility. Several origins for the intermediate intensity fog droplets have been proposed, including abnormal negative droplets, merged positive and negative droplets, fragmented droplets, amplification of nontarget sequences, inhibited amplification, and delayed onset of amplification.[6,14,15] These differing proposals impact how droplets should be classified or even counted. Misclassification of fog droplets has been identified as the most significant source of bias in ddPCR assays.[16]

With any given ddPCR assay, establishing an unbiased estimate of λ therefore requires identifying which of these proposed mechanisms significantly contribute to the fog. The pBR322 plasmid is a model system for demonstrating a connection between cdPCR late starts and ddPCR fog. Figure 1A displays the large fraction of late-start reaction curves observed with the native supercoiled form of the plasmid using the 1332 assay with the GE master mix. Improving accessibility by enzymatically opening the circular plasmid (Figure 1B) or using the MZ master mix which contains a (proprietary) amplification enhancer (Figure 1C) essentially eliminates late starts.

There currently is no master mix equivalent to MZ available for our ddPCR system. Figure 2 compares just the ddPCR evaluation of supercoil and linearized plasmid using the "no dUTP" supermix. With this mastermix, there were no nonnegative droplets in any nontemplate control (NTC) sample. (This was not the case with an alternate master mix for our system, an indication of reagent contamination and a reminder that assay specificity can vary between platforms and their reagents.)

Given that both linearization and the use of an amplification enhanced mastermix in cdPCR eliminate late starts, the vast reduction in droplet fog with the linearized plasmid indicates that cdPCR late starts and ddPCR fog have a common source: target accessibility.

In our hands, λ for MZ-amplified supercoil pBR322 was 4% larger than for the MZ-amplified linearized plasmid with both the 1332 assay (see Supporting Information Figure S1) and another independent assay (data not shown). This suggests that the linearization process may have rendered some targets nonamplifiable. This is in accord with previous work with human genomic DNA showing that, while enzymatic restriction can dramatically improve target accessibility, it may also reduce the number of amplifiable targets.[12] While complicating accurate quantitation, this potential target damage does not affect the utility of the linearized plasmid for comparing platform performance since the same samples are used in both systems.

Platform Concordance. Since $C = \lambda/(FV)$, if two dPCR systems (call them "A" and "B") are concordant, then for a given sample $CF = \lambda_A/V_A = \lambda_B/V_B$. Given that the linearized pBR322 plasmid appears to be fully accessible in both cdPCR and ddPCR, a split-sample comparison of λ across a dilution series addresses whether there is intrinsic bias between the platforms. This direct comparison of samples is possible because the ≈25% difference between the manufacturers' stated volumes for the 48.770 cdPCR chambers and QX200 ddPCR droplets is not significant given the dynamic range of the two platforms. Comparisons involving platforms with significantly different partition volumes would require using different sample dilutions in the two systems, introducing an additional source of variability.

The relatively small number of cdPCR partitions per replicate measurement (770 chambers per panel versus 10 000−20 000 droplets per ddPCR well) limits direct split-sample comparisons to λ between about 0.005 and 4 targets per partition. Figure 3 demonstrates that over this nearly 3-order-of-magnitude range the λ from the two platforms are linearly related.

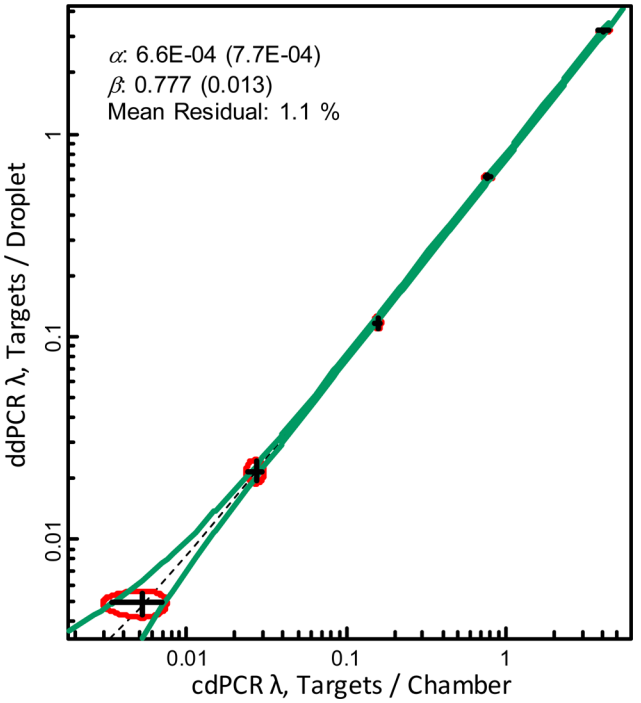

Figure 3. Split-sample comparison of cdPCR and ddPCR results. The samples were designed to yield λ spanning nearly 3 orders of magnitude. The black crosses are the mean and 95% expanded uncertainties for cdPCR and ddPCR λ estimates for technical replicates of a set of linearized pBR322 plasmid samples. The red ellipses are 95% confidence bounds on the joint distribution of the {cdPCR, ddPCR} λ. The dashed black line represents the errors-in-variables linear regression line. The bordering green lines represent the 95% confidence bounds on the regression line. The legend lists the intercept (α) and slope (β) parameter values and their standard (1σ) uncertainties.

The relationship documented in Figure 3 was parametrized using an errors-in-variables regression technology that considers the measurement imprecision of both platforms.[17] The uncertainties on the slope and intercept and the line's 95% confidence interval were estimated using parametric bootstrap Monte Carlo analysis.[18] This model provides a satisfyingly small mean absolute relative residual of just over 1%. Importantly, the absolute value of the intercept is smaller than its standard uncertainty.

While not relevant to establishing the traceability of ddPCR results, the slope of the regression model is proportional to the relative volumes of the reaction partitions of the two platforms: since $CF = \lambda_A/V_A = \lambda_B/V_B$, then $V_B/V_A = \lambda_B/\lambda_A$. We are currently investigating whether this could provide a metrologically sound approach to estimating chamber volume.

DOI: 10.1021/acs.analchem.7b00240
Anal. Chem. 2017, 89, 4648−4654

While the linearity of the relationship between the two platforms needs to be established for new assays and sample types, this split-sample analysis demonstrates that, within the measurement uncertainties, ddPCR results are intrinsically concordant with cdPCR results over the cdPCR working range.

Classifying the Fog. Some of the nominally positive droplets at the bottom of the left-hand bins of Figure 2 cluster around discrete values, forming bands. We believe that these bands reflect successive one-cycle amplification delays and, in analogy to the rt-cdPCR curves in Figure 1A, would continue to rise from the low-intensity "negative" band regardless of the number of amplification cycles.

Figure 4 is a high-resolution display of results for the 22C3 assay of NIST2 human genomic DNA after 25 cycles, just past

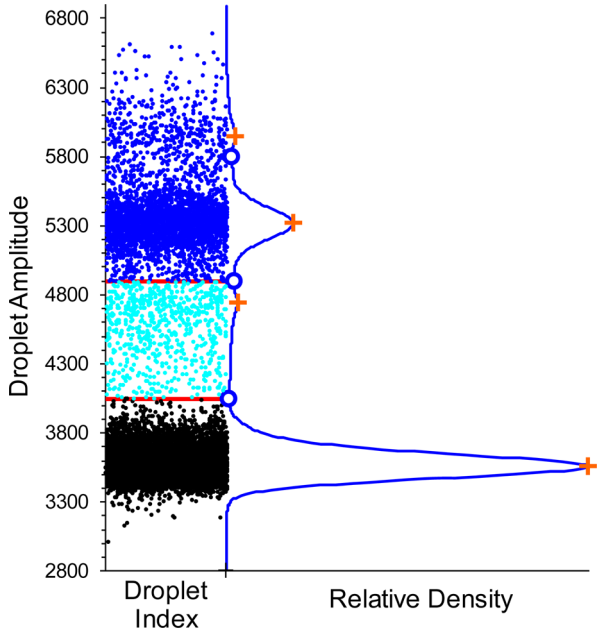

Figure 4. ddPCR fluorescence intensity for the 22C3 assay of NIST2 human genomic DNA at a 25-cycle end point. Black specks at the bottom denote negative droplets, blue specks at the top denote positive droplets, and the cyan specks in between denote the intermediate intensity fog droplets. The curve to the right is the probability density function (PDF) of the droplet distribution. The open blue circles mark the minima of the PDF used to classify the droplet signals, with red lines marking the boundaries between the three classes. The red crosses mark the PDF maxima.

the rt-cdPCR Ct for this sample with this assay. The lightly smoothed empirical probability density function (PDF) of droplet intensities shown to the right of the droplets facilitates systematic classification of droplets as negative, fog, and positive. Droplets of intensity less than the first minimum immediately above the lowest peak are negative. Droplets of intensity greater than the last minimum immediately below the main upper peak are positive. Droplets of intensity between these minima are fog.

In contrast to the multiple thin bands of the supercoil plasmid, with the well-behaved NIST2 material and 22C3 assay there is a single rather diffuse band of intermediate intensity droplets within the fog that is more easily visualized as a small PDF peak. This peak is analogous to the final plateau in cdPCR Ct ogives attributed to targets that begin amplifying one cycle late.[7] There is also a small PDF peak just above the main band of positive droplets that is analogous to the two-target shoulder in some cdPCR ogives[7] (see the NEIF ogive in Supporting Information Figure S4.)

Figure 5 displays results for the 22C3 assay of NIST2 aliquots at end points of 25, 30, 35, 40, 50, 60, 80, and 110

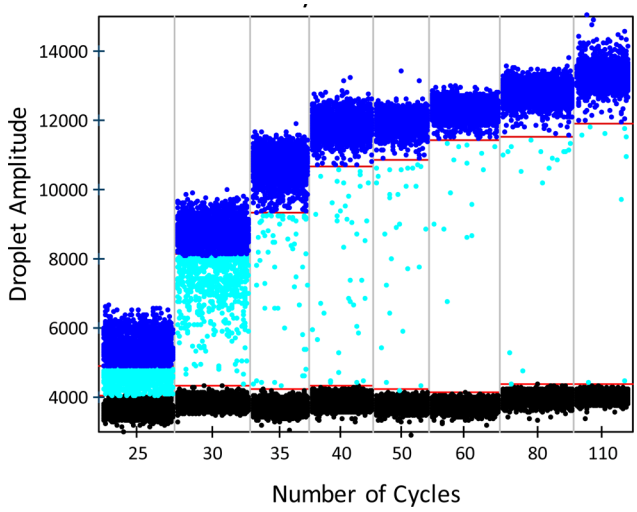

Figure 5. ddPCR fluorescence intensity for the 22C3 assay of NIST2 human genomic DNA as a function of end point amplification cycle number. Black specks denote negative droplets. Blue specks denote unambiguously positive droplets. Cyan specks denote fog. The red horizontal lines represent the thresholds used to classify the droplets. The gray vertical lines bound the combined results of four technical replicates of each individual sample.

cycles. The results were collected in eight separate ddPCR experiments conducted over 48 days. Nearly all of the fog droplets have lifted well above the negatives by the 60-cycle end point. While the intensity of the positive droplets continues to increase with additional cycles, after 60 cycles so does the intensity of the negative droplets, keeping the separation between the negative and positive droplets approximately constant. Supporting Information Figure S5 documents that the ND6, NEIF, and NR4Q assays yielded very similar results.

Quantification of End Point Results. Figure 6 summarizes the proportion of positive, fog, and negative droplets as functions of cycle end points for the 22C3, ND6, NEIF, and NR4Q assays. The proportion of fog droplets continues to fall until reaching an apparent plateau of about 0.2% by 80 cycles. However, within the limits of the measurement variability, the proportion of negative droplets does not appreciably change after 40−50 cycles.

Figure 7 displays the estimated λ when the fog droplets are reclassified as positive. For all four assays, λ is effectively independent of end point cycle once the fog has lifted above the negative band. Supporting Information Table S4 lists the λ values and statistical summaries.

The relative standard uncertainty of the 20 results for end points of 40 or more cycles shown in Figure 7 is 1.1%. This estimate combines between-assay, -end point, -cartridge, and -day variability. While slightly asymmetric about the best fit sigmoidal curve, the relative standard uncertainty of the estimated asymptote is 0.5%. While a bias, the 0.2% residual fog is small relative to the analytical imprecision. Note that these estimates are specific to a specific dilution of the NIST2 sample.

DOI: 10.1021/acs.analchem.7b00240
Anal. Chem. 2017, 89, 4648−4654

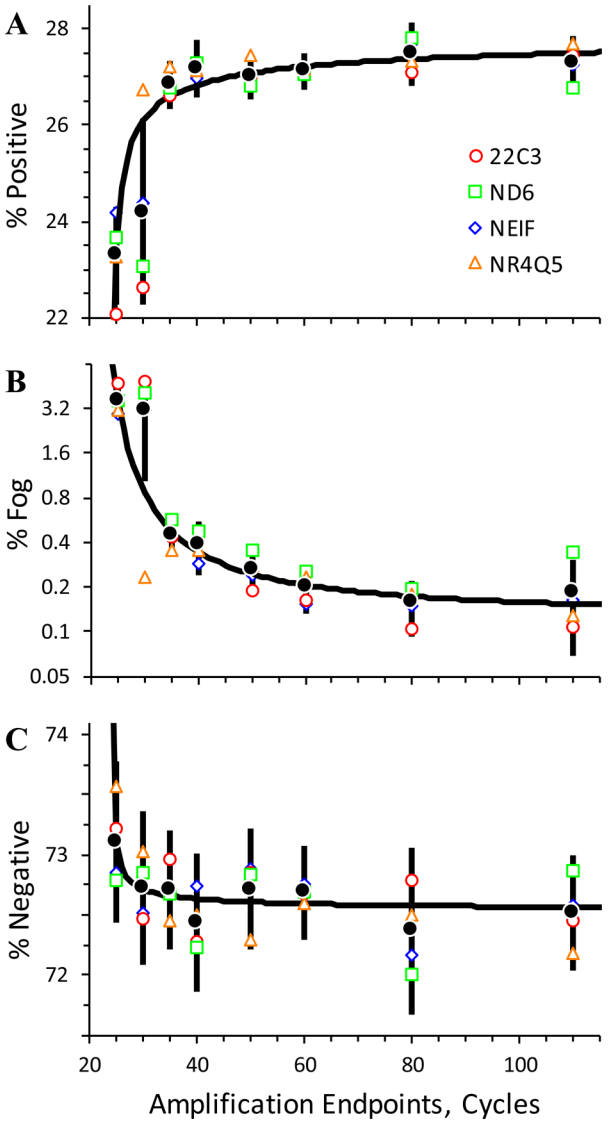

Figure 6. Percent positive (A), fog (B), and negative (C) droplets as functions of end point cycle. Each open symbol represents the mean percent for four technical replicates of a given assay at a given end point. The solid circles and bars represent the mean and standard deviation of the four assays at that end point. The black curves represent empirical sigmoidal fits to the data.

Extending the end point beyond the recommended ≈40 cycles[19] is expensive in terms of analysis time but has little or no adverse effect on λ. At least through 80 cycles, it also has little effect on the total number of droplets, N_{tot} (see Supporting Information Figure S6.)

Multiple Assays. Any single assay could be incompletely selective and coamplify one or more secondary targets or could be insensitive to some conformations of a target-containing DNA fragment. Therefore, establishing quantitative agreement among several independent assays is essential for establishing metrological traceability. The greater the number of independently developed and validated assays that give the same result for multiple independent samples, the stronger the traceability argument. The four human genomic assays discussed here (Figures 6 and 7) were developed and optimized for unique targets on separate chromosomes.

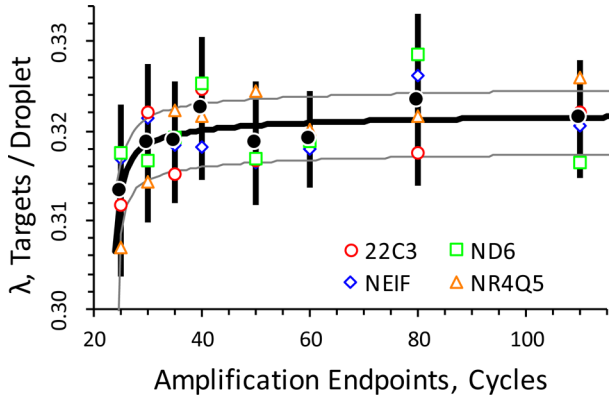

Figure 7. Targets per droplet, λ, as a function of end point cycle. Each open symbol represents the mean λ for four technical replicates of a given assay at a given end point. The solid circles and bars represent the mean and standard deviation of λ for the four assays at that end point. The thick black curve represents an empirical sigmoidal fit to the data; the thin gray curves represent an approximate 95% confidence interval on the sigmoid.

CONCLUSIONS

Metrological traceability is essential and indispensable for the certification of results delivered by any CRM. Prior to the development of direct counting[11,20] and dPCR techniques, quantifying DNA required calibration to some appropriate material or data standard.[21] While fit for transferring traceability to reference materials intended for routine use, calibration to a reference of the same kind is not acceptable for certifying a value for a primary measurement standard.[2]

Several national metrology institutes besides our own have devoted considerable resources to establishing the metrological utility of various dPCR platforms for DNA quantification applications.[5,22,23] As with other measurement systems, demonstrating that a platform can provide accurate and traceable results with one application does not demonstrate that other applications will achieve such results.

To traceably establish target concentration using dPCR, traceability must be established for three quantities: λ, the number of targets per partition volume, F, the dilution factor, and V, the partition volume. The manufacturers of the dPCR systems we use do not specify partition volume in a metrologically adequate manner: at minimum, a value and associated 95% uncertainty. In the absence of such specification, establishing formal traceability for a primary DNA quantification standard requires the certifying body to themselves establish V. Further, since partition volumes may vary between microfluidic device batches and reagent lots, V ideally should be determined using the same materials and reagents used to establish λ. At this time, we have this capability only for droplets produced by the QX200 system.

We argue here that results from rt-cdPCR systems can be used to directly validate several of the critical end point assay requirements. With cdPCR systems, spatial evaluation of the distribution of positive and negative chambers enables confirming random segregation. With rt-cdPCR systems, the shape of the amplification curves and the distribution of their Ct values enables assessing whether all positive chambers contained a target of interest and whether the targets segregated independently in accord with Poisson expectation.

Therefore, we believe that establishing formal metrological traceability for a system of ddPCR assays with a particular type

DOI: 10.1021/acs.analchem.7b00240
Anal. Chem. 2017, 89, 4648−4654

of sample at this time requires use of both ddPCR and rt-cdPCR. If cdPCR λ results for a given system are established as traceable, then a series of validation studies can establish the formal concordance of the cdPCR and ddPCR λ determinations: (1) If present, ddPCR fog droplets must be correctly classified. If the amplification curves of cdPCR late-start positive chambers have the expected shape, the common origin of fog and late starts can be established if fog decreases with increased accessibility. Use of PCR enhancers, comparison of native and enzyme-digested samples, and split-sample measurements at 30, 40, 60, and 80 cycles can (a) establish whether the fog mostly results from target inaccessibility and (b) estimate the proportion of any residual fog that must be treated as a bias. (2) Direct split-sample comparison of ddPCR and cdPCR λ results over the cdPCR working range (for the 48.770 platform, about 0.005−4 λ) are required. If the ddPCR results are linearly related to the cdPCR results and the 95% level of confidence interval on the relationship's intercept includes zero, the ddPCR λ inherit the traceability established by rt-cdPCR. (3) Three or more independent assays must provide consistent (identical within long-term intermediate imprecision) estimates of λ. At least one of these assays must efficiently amplify the target sequence in the original DNA and in the first- and second-generation amplicons.[7] The assay targets should be well-separated; for human DNA, ideally the targets should be on different chromosomes.

When the sample dilution factor F is realized using properly calibrated volumetric and gravimetric devices and the ddPCR λ and droplet V are traceably established, a ddPCR estimate of target concentration C becomes formally traceable to the SI.

■ ASSOCIATED CONTENT

Supporting Information

The Supporting Information is available free of charge on the ACS Publications website at DOI: 10.1021/acs.analchem.7b00240.

Protocols, tables, figures, and dMIQE (PDF)

cdPCR and ddPCR CSV files used in figures (ZIP)

■ AUTHOR INFORMATION

Corresponding Author

*E-mail: david.duewer@NIST.gov. Phone: 301-975-3935. Fax: 301-926-8671.

ORCID

Margaret C. Kline: 0000-0003-2796-1998

David L. Duewer: 0000-0002-3924-3064

Author Contributions

The manuscript was written with contributions of both authors. Both authors have given approval to the final version of the manuscript.

Notes

Certain commercial equipment, instruments, or materials are identified in this report to specify adequately experimental conditions or reported results. Such identification does not imply recommendation or endorsement by the National Institute of Standards and Technology, nor does it imply that the equipment, instruments, or materials identified are necessarily the best available for the purpose.

The authors declare no competing financial interest.

■ ACKNOWLEDGMENTS

This work was supported in part through the NIST Special Programs Office.

■ REFERENCES

(1) de St. Groth, S. F. *J. Immunol. Methods* **1982**, *49* (2), R11−R23.

(2) JCGM 200:2012 International vocabulary of metrology—Basic and general concepts and associated terms (VIM). Joint Committee for Guides in Metrology, Sevres, France, 2012. www.bipm.org/en/publications/guides/vim.html (Accessed April 3, 2017).

(3) Fischer, J.; Ullrich, J. *Nat. Phys.* **2016**, *12*, 4−7.

(4) De Bièvre, P.; Dybkaer, R.; Fajgelj, A.; Hibbert, D. B. *Pure Appl. Chem.* **2011**, *83* (10), 1873−1935.

(5) Deprez, L.; Corbisier, P.; Kortekaas, A. M.; et al. *Biomol. Det. Quant.* **2016**, *9*, 29−39.

(6) Witte, A. K.; Mester, P.; Fister, S.; et al. *PLoS One* **2016**, *11* (12), e0168179.

(7) Duewer, D. L.; Kline, M. C.; Romsos, E. L. *Anal. Bioanal. Chem.* **2015**, *407* (30), 9061−9069.

(8) Jacobs, B. K. M.; Goetghebeur, E.; Clement, L. *BMC Bioinf.* **2014**, *15*, 283.

(9) Bhat, S.; Herrmann, J.; Armishaw, P.; et al. *Anal. Bioanal. Chem.* **2009**, *394* (2), 457−467.

(10) Dagata, J. A.; Farkas, N.; Kramer, J. A. *Method for Measuring the Volume of Nominally 100 μm Diameter Spherical Water-in-Oil Emulsion Droplets*; NIST Special Publication 260-184; National Institute of Standards and Technology: Washington, DC, 2016. DOI: 10.6028/NIST.SP.260-184.

(11) Yoo, H.-B.; Park, S.-R.; Dong, L.; et al. *Anal. Chem.* **2016**, *88* (24), 12169−12176.

(12) Kline, M. C.; Romsos, E. L.; Duewer, D. L. *Anal. Chem.* **2016**, *88* (4), 2132−2139.

(13) Dong, L.; Yoo, H. B.; Wang, J.; Park, S.-R. *Sci. Rep.* **2016**, *6*, 24230.

(14) Trypsteen, W.; Vynck, M.; De Neve, J.; et al. *Anal. Bioanal. Chem.* **2015**, *407* (19), 5827−5834.

(15) Gerdes, L.; Iwobi, A.; Busch, U.; Pecoraro, S. *Biomol. Det. Quant.* **2016**, *7*, 9−20.

(16) Jacobs, B. K.; Goetghebeur, E.; Clement, L. *BMC Bioinf.* **2014**, *15*, 283.

(17) Ripley, B. D.; Thompson, M. *Analyst* **1987**, *112*, 377−383.

(18) Duewer, D. L.; Gasca-Aragon, H.; Lippa, K. A.; Toman, B. *Accredit. Qual. Assur.* **2012**, *17* (6), 567−588.

(19) QX200 Droplet Reader and QuantaSoft Software Instruction Manual, Catalog Nos. 186-4001, 186-4003. www.bio-rad.com/webroot/web/pdf/lsr/literature/10031906.pdf (Accessed April 3, 2017).

(20) Lim, H.-M.; Yoo, H.-B.; Hong, N.-S.; et al. *Metrologia* **2009**, *46*, 375−387.

(21) Bhat, S.; Curach, N.; Mostyn, T.; et al. *Anal. Chem.* **2010**, *82* (17), 7185−7192.

(22) Devonshire, A. S.; Honeyborne, I.; Gutteridge, A.; et al. *Anal. Chem.* **2015**, *87* (7), 3706−3713.

(23) Bhat, S.; Emslie, K. R. *Biomol. Det. Quant.* **2016**, *10*, 47−49.

DOI: 10.1021/acs.analchem.7b00240
Anal. Chem. 2017, 89, 4648−4654